ARTICLE IN PRESS

NRIAG Journal of Astronomy and Geophysics xxx (xxxx) xxx–xxx

Contents lists available at ScienceDirect

NRIAG Journal of Astronomy and Geophysics

journal homepage: www.elsevier.com/locate/nrjag

Full length article

Using RTK and VRS in direct geo-referencing of the UAV imagery

M. Rabah[a,*], M. Basiouny[a,b], E. Ghanem[a], A. Elhadary[a]

[a] Department of Civil Engineering, Benha Faculty of Engineering, Benha University, Egypt
[b] Department of Civil Engineering, Faculty of Engineering, Egyptian Chinese University (ECU), Egypt

ARTICLE INFO

Keywords:
UAV photogrammetry
UAV imagery
Direct Geo-referencing
DG

ABSTRACT

Direct Geo-Referencing is a new technique in photogrammetry, especially in the aerial photogrammetry. Unlike the Aerial Triangulation "AT", this method does not require Ground Control Points "GCPs", to process aerial photographs into desired ground coordinates systems. Compared with the old method, this method has four main advantages: faster field work, faster data processing, simple workflow and less cost. Generally, direct geo-referencing using two systems, Global Navigational Satellite Systems "GNSS" and Inertial Navigational System "INS". GNSS recording the camera coordinates "X, Y, Z", and INS recording the camera orientation angles "*w*, φ, *k*" at the time of exposure. These parameters merged and are provided to each photograph in the processing stage.

The current paper investigates the using GNSS system for providing the linear exterior orientation "EO" parameters "X, Y, Z" by two techniques, real time kinematic "RTK" and virtual reference system "VRS". The accuracy of the applied method is tested on topographic survey project in Switzerland. The surveyed data of the specified project were collected by amateur digital camera Canon 18.2 MP, 182 captured images from approximately 85 m flight height, 18 Ground Check Point "GCP" determined by static GNSS. Horizontal accuracy is 0.029 m for VRS case, 0.034 m for RTK case and vertical accuracy is 0.026 m for VRS case, 0.029 for RTK case.

1. Introduction

Aerial photogrammetry is one of the most appropriate ways of data acquisition in producing large-scale topographical maps. Geo-referencing technique for Traditional aerial photogrammetry, called aerial triangulation "AT", is depending mainly on Ground Control Points "GCPs". This technique has many disadvantages and caused to many areas have not basic topographical maps due to lacking GCPs or inaccessible areas (Li, 2005).

Unlike AT, Direct Geo-referencing "DG", see Fig. 1, is the direct position and orientation measurements of the camera during capturing so, each pixel can be geo-referenced to the Earth coordinate system without any needing for ground information. Development in GNSS/INS technology made a great rebound in digital photogrammetry. GNSS records coordinate "X, Y, Z" and INS records orientation angles "w, φ, k" at the time of exposure. These measurements are integrated and form six parameters which are called Exterior Orientation "EO" parameters, that are used in collinearity equation for Geo-referencing (Cramer et al., 2000). In a traditional photogrammetry, EO parameters are produced from Aerial Triangulation "AT" which needs Ground Control Points "GCPs" distributed regularly. The benefits of Direct Geo-referencing can be summarized as follows:

- Cost savings by elimination of needing GCPs in the field.
- Ability to generate remote locations maps.
- Real-time mapping for disaster response Applications.
- Eliminating or at least reducing side-lap requirements causing fewer flight lines per area.

In direct geo-referencing, exterior orientation parameters are computed through Kalman filter applied over the GNSS and INS observations. The errors of GNSS, time synchronization and Centre deviation between GNSS and camera may cause errors in linear exterior orientation parameters. In the same way, attitude measurement errors in INS may cause errors in angular exterior orientation parameters (Jacobsen, 2002). In direct geo-referencing, experiments appeared that the errors caused by angular parameters are larger than errors caused by linear parameters, and they are the most effect in direct geo-referencing errors (Cramer and Stallmann, 2002).

In the current paper, the accuracy of DG by using only linear exterior orientation parameters determined by real time kinematic "RTK" and virtual reference system "VRS" techniques is investigated, the

Peer review under responsibility of National Research Institute of Astronomy and Geophysics.
* Corresponding author.
E-mail address: mrabah@bfe.bu.edu.eg (M. Rabah).

https://doi.org/10.1016/j.nrjag.2018.05.003
Received 22 February 2018; Received in revised form 8 April 2018; Accepted 19 May 2018
2090-9977/ © 2018 Published by Elsevier B.V. on behalf of National Research Institute of Astronomy and Geophysics This is an open access article under the CC BY-NC-ND license (http://creativecommons.org/licenses/BY-NC-ND/4.0/).

Please cite this article as: Rabah, M., NRIAG Journal of Astronomy and Geophysics (2018), https://doi.org/10.1016/j.nrjag.2018.05.003

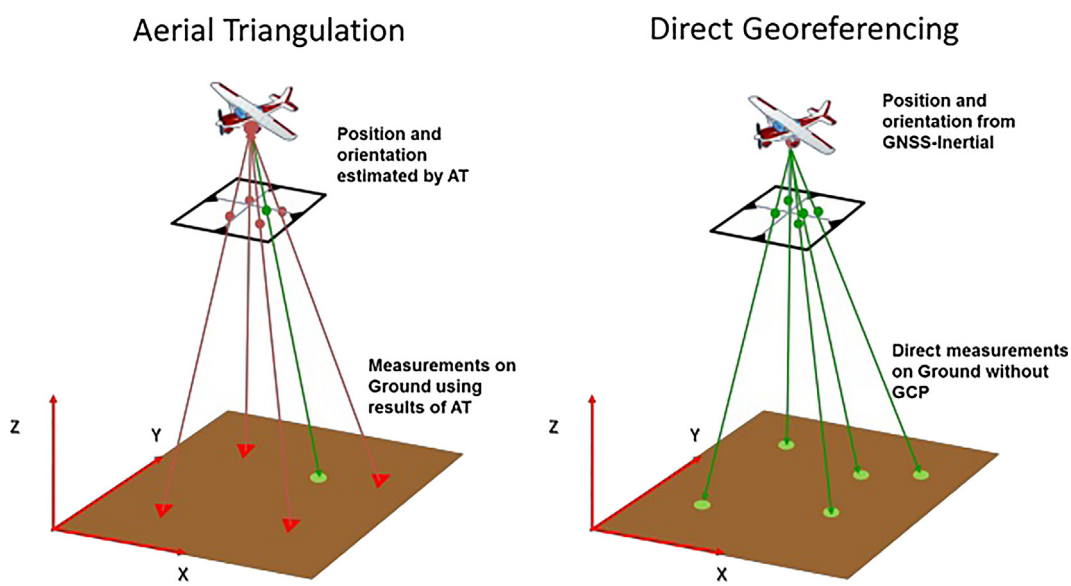

Fig. 1. Direct geo-referencing and aerial triangulation concept.

angular exterior orientation parameters are calculated in Structure from Motion "SFM" approach.

2. Research methodology

2.1. Area of study

Our test area is in Switzerland where (latitude = 46.59709187°, longitude = 6.608701005°, altitude = 668.8272854 m), Fig. 2 shows the study area in google maps. In general, the test site covered approximately 0.827 km^2.

2.2. Data acquisition

In 21/8/2014, flight data acquisition of a height approximately 85 m above ground level has been performed using a fixed wing UAV eBee with wingspan 960 mm to photograph the test area, characteristics of the UAV are shown in Table 1 and Fig. 3 shows the shapes of UAV and camera used. This medium altitude has been performed to minimize the data time acquisition, data processing and get suitable ground

Table 1
Characteristics of the eBee RTK UAV.

Dimensions	55 × 45 × 25 cm
Weight	0.73 kg
Wing span	96 cm
Material	EPP foam and carbon
GNSS/RTK receiver	L1, L2, GPS, GLONASS
Camera	Wx "18.2 MP"
Max. flight time	40 min
Speed	40–90 km/hr.
Max. coverage "in one flight"	8 km^2
Wind resistance	Up to 45 km/hr
GSD	Down to 1.5 cm per pixel

Fig. 2. The area study on the google map.

Fig. 3. Fixed wing UAV and camera used.

sample distance "GSD".

This acquisition captured 182 full-color aerial images with 80% overlap and 80% side-lap which are sufficiently for processing by using the photogrammetric approach. 18-ground control and check points are distributed and determined by static post processing. In other side, the linear exterior orientation parameters for each photograph were determined by real time kinematic "RTK" and virtual reference system "VRS" techniques in World Geodetic System 1984 "WGS84".

2.3. Data processing

Agisoft Photo Scan is one of the most accurate photo processing software which is used to apply SFM approach. It implements feature matching algorithm on the photographs. Firstly, it detects points in the images which are captured from different viewing and lighting sources then descript their points. Finally, the descriptors of the points are used for object reconstruction across the successive images (Agisoft, 2017). The linear exterior orientation parameters are read from Exchangeable Image File Format "EXIF". The 3D model in an absolute coordinate has been created from pairs of images. The Agisoft photo scan has a good geometric accuracy, cost and ease of use (Gross, 2015; Gross and Heumann, 2016). The processing parameters of Agisoft are shown in Table 2.

3. Results and discussions

Direct Geo-referencing does not need any GCPs. So, all GCPs are changed to Independent Check Points "ICP" which used for to checking the accuracy of this method. RMSE are calculated by using SFM approach to measure GCPs coordinates "from models generated by linear EO parameter from GNSS" and compare them to original coordinates from static GNSS assumed as true value.

Table 2
The processing parameters defined in Agisoft SW.

No. of images	182
No. of ground points	18
Coordinate system	WGS 84 "EPSG 4326"
Key points	40,000
Tie points	10,000
Optimization parameters	F, cx, cy, b1, b2, k1, k2, k3, p1, p2
Pixel size	1.34 × 1.34 µm
Resolution	4608 × 3456
Camera model	CanonIXUS127HS "4.3 mm" 4608 × 3456
Focal length	4.3 mm
Ground resolution	2.59 cm/pix
Flying altitude	84.7 m
Coverage area	0.827 km^2

Where:
F: Focal length.
cx & cy: Principal point coordinates.
b1 & b2: Affinity and Skew transformation coefficients.
k1, k2 & k3: Radial distortion coefficients.
p1 & p2: Tangential distortion coefficients.

RMSE is calculated for check points in the different between the UAV data and the reference data "static GNSS" (FGDC, 1998):

$$RMSE_X = \sqrt{\frac{\sum (X_{GNSS} - X_{UAV})^2}{n}}$$

$$RMSE_Y = \sqrt{\frac{\sum (Y_{GNSS} - Y_{UAV})^2}{n}}$$

$$RMSE_{XY} = \sqrt{{RMSE_X}^2 + {RMSE_Y}^Y}$$

$$RMSE_Z = \sqrt{\frac{\sum (Z_{GNSS} - Z_{UAV})^2}{n}}$$

Evaluation the model by using limited check points number is not enough. So, using all model points in evaluation is more suitable, this evaluation was expressed by using the multi-scale model to model comparison "M3C2" technique which is a plugin in the open source cloud compare software which has most accurate technique for point clouds change detection (Barnhart and Crosby, 2013). For this method the point clouds from DG are compared by the AT point clouds "assumed as a true value and a reference".

3.1. Study the accuracy of Aerial Triangulation "AT"

18 ground points are measured by static GNSS. 10 points are used as GCPs and distributed in all area, the other 8 points are used as a check points. Fig. 4 show the position of the GCPs and the check points.

Accuracy of point clouds and Digital Surface Model "DSM" derived by AT process can be derived by comparing it with check points derived from static GNSS, as threshold values. The differences between the static GNSS check points and the related points in the point clouds are given in Table 3.

As it is shown in Table 3 and Fig. 5, one can easily conclude that the elevation and northing RMSE values are higher than Easting RMSE. Horizontal and Vertical errors have approximately the same RMSE. The maximum & the minimum values of horizontal error are 0.022 & 0.001 and for vertical error are 0.026 & 0.00002 m.

3.2. Study the accuracy of the Direct Geo-referencing "DG"

The three linear exterior orientation parameters are determined by GNSS instead of calculated by AT in SFM approach. Two techniques of accurate differential Global Navigational Satellite Systems "DGNSS" are used, RTK and VRS.

3.2.1. Study the accuracy of Direct Geo-referencing using RTK in determining linear exterior orientation parameters

The linear EO parameters was determined by RTK, the angular EO was derived from AT. All 18-ground control points was used as a check points. Fig. 6 shows the check points locations.

Accuracy of point clouds and DSM derived by RTK-DG process can be derived by comparing it with the check points derived from static

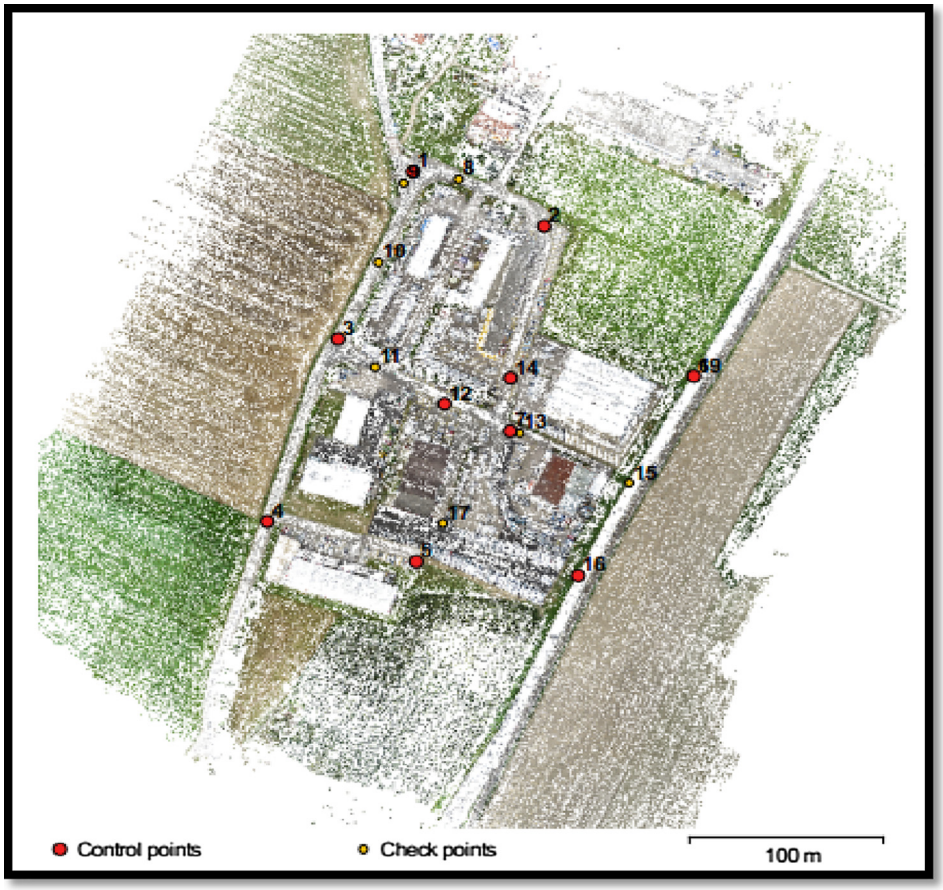

Fig. 4. The GCPs and the check points locations.

Table 3
Errors & RMSE of check points for AT process case.

Points	Easting error (m)	Northing error (m)	Horizontal error (m)	Vertical error (m)	Total error (m)
point8	−0.0004	0.007	0.007	−0.008	0.010
point9	0.005	0.021	0.022	0.00002	0.022
point10	0.0001	−0.008	0.008	0.026	0.029
point11	−0.010	−0.018	0.021	−0.006	0.022
point13	−0.004	−0.017	0.017	0.015	0.023
point15	0.001	−0.0008	0.001	0.013	0.013
point17	0.006	0.004	0.007	−0.013	0.015
point19	−0.0006	0.009	0.009	−0.0007	0.009
Total RMSE	0.006	0.013	0.014	0.013	0.019

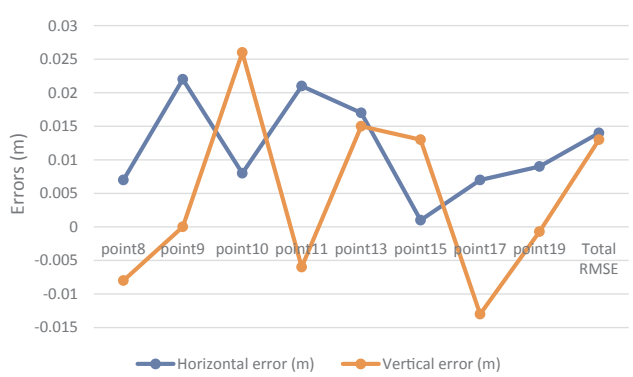

Fig. 5. The differences between the check points and related point clouds produced by AT.

GNSS. The differences between both sets of points were computed and output in Table 4. As it is seen in Table 4 and Fig. 7, horizontal error is higher than vertical error in most of the check points. The maximum & the minimum absolute values of horizontal error are 0.065 & 0.007 m. and for vertical error are 0.061 & 0.003 m.

The differences between the point clouds derived by RTK-DG process of linear EO and the point clouds derived from AT process are computed and plotted in the histogram depicted in Fig. 8.

As it is illustrated in Fig. 8, we found that 90% of the differences locates between (−0.08 to 0.04) m, 75% of the differences locates between (−0.06 to 0.04) m, the mean of the differences equals 0.0304 m with standard deviation 0.0398 m. The given results reveal that RTK-DG can achieve centimeters accuracy in horizontal and vertical.

3.2.2. Study the accuracy of direct geo-referencing using VRS in determining linear exterior orientation parameters.

The linear EO parameters were determined by VRS, the angular EO was determined from AT. All 18-ground control points was used as a check points, Fig. 6 shows the check points locations. Accuracy of point clouds and DSM derived by VRS-DG process can be derived by compare it with check points derived from static GNSS. The differences between the DSM derived by VRS-DG and the related check points derived from static GNSS are demonstrated in Table 5 and Fig. 9.

As it is illustrated in Table 5 and Fig. 9, it is easily to see that Horizontal RMSE is higher than Vertical RMSE. The maximum & the minimum absolute values of horizontal error are 0.052 & 0.007 m and for vertical error are 0.045 & 0.007 m. To see the overall accuracy of point clouds derived by VRS-DG process we compared it with point clouds derived from AT process. The differences between the point clouds derived by VRS-DG process of linear EO and the point clouds

Fig. 6. Check points locations.

Table 4
Errors & RMSE of check points for RTK-DG case.

points	Easting error (m)	Northing error (m)	Horizontal error (m)	Vertical error (m)	Total error (m)
point1	0.0003	−0.037	0.037	−0.021	0.043
point2	−0.040	−0.016	0.043	−0.003	0.043
point3	0.019	0.001	0.019	0.005	0.019
point4	−0.030	0.056	0.064	−0.005	0.064
point5	0.024	0.009	0.026	−0.043	0.050
point6	−0.011	−0.0009	0.011	−0.016	0.020
point7	−0.063	0.014	0.065	−0.046	0.079
point8	−0.013	−0.023	0.026	−0.013	0.030
point9	0.005	−0.009	0.010	−0.013	0.016
point10	0.018	−0.011	0.021	0.008	0.023
point11	−0.009	−0.008	0.012	−0.014	0.019
point12	−0.024	0.029	0.038	−0.017	0.042
point13	−0.024	−0.008	0.025	−0.021	0.033
point14	0.006	0.003	0.007	−0.024	0.025
point15	−0.022	0.011	0.025	−0.041	0.048
point16	−0.038	0.024	0.045	−0.052	0.068
point17	−0.010	0.031	0.033	−0.061	0.069
point19	−0.027	0.011	0.029	−0.020	0.035
Total RMSE	0.026	0.022	0.034	0.029	0.045

derived from AT process are computed and plotted in the histogram depicted in Fig. 10.

As it is shown in Fig. 10, 90% of the differences locates between (−0.07 to 0.04) m, 75% of the differences locates between (−0.05 to 0.025) m, the mean of the differences equals 0.0278 m with standard deviation 0.0348 m. This result reveals that VRS-DG can achieve centimeter accuracy in horizontal and vertical.

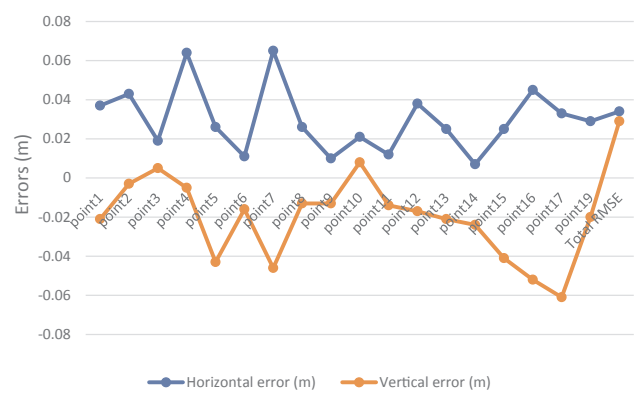

Fig. 7. The differences between the point clouds derived by RTK-DG and the point clouds derived from AT process.

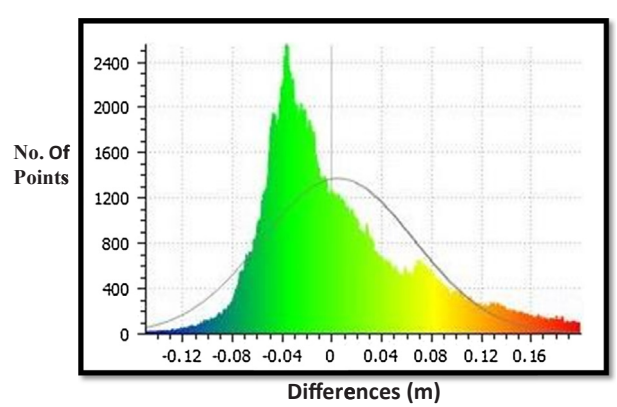

Fig. 8. Change detection of point clouds model between AT and RTK-DG.

Table 5
Errors & RMSE of check points for VRS-DG case.

points	Easting error (m)	Northing error (m)	Horizontal error (m)	Vertical error (m)	Total error (m)
point1	0.0064	−0.031	0.032	−0.029	0.043
point2	−0.028	−0.009	0.029	−0.011	0.031
point3	0.027	−0.002	0.027	0.009	0.029
point4	−0.010	0.051	0.052	0.009	0.052
point5	0.040	0.009	0.041	−0.028	0.050
point6	0.005	0.005	0.007	−0.016	0.017
point7	−0.047	0.017	0.050	−0.045	0.067
point8	−0.005	−0.016	0.017	−0.024	0.030
point9	0.010	−0.004	0.011	−0.018	0.022
point10	0.024	−0.012	0.027	0.012	0.029
point11	0.001	−0.010	0.010	−0.011	0.015
point12	−0.012	0.029	0.031	−0.007	0.032
point13	−0.008	−0.004	0.009	−0.021	0.022
point14	0.021	0.007	0.022	−0.026	0.034
point15	−0.005	0.016	0.017	−0.040	0.043
point16	−0.022	0.027	0.035	−0.038	0.051
point17	0.004	0.031	0.031	−0.044	0.054
point19	−0.011	0.017	0.020	−0.020	0.028
Total RMSE	0.020	0.021	0.029	0.026	0.039

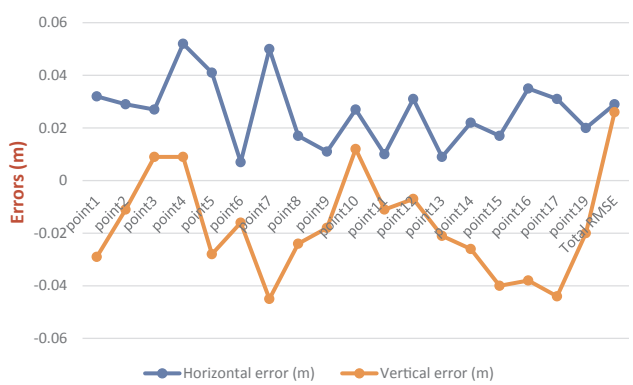

Fig. 9. The differences between the point clouds derived by VRS-DG and the point clouds derived from AT process.

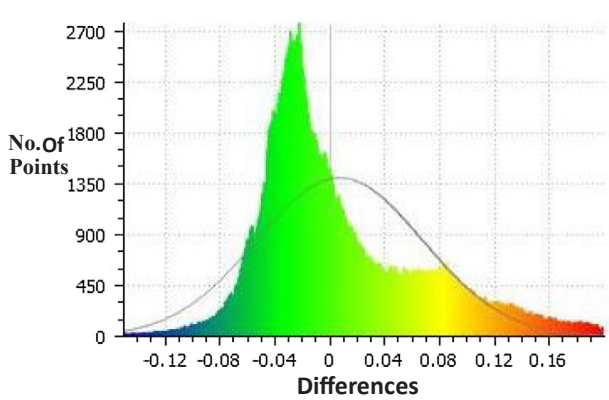

Fig. 10. Change detection of Point clouds model between AT and VRS-DG.

3.3. Relation between accuracy of AT and DG by linear EO parameters determined by RTK and VRS techniques

For evaluating the point clouds extracted by RTK-DG, the point clouds extracted by VRS-DG against the point cloud extracted by AT, the total RMSE for eight check points are computed by the three methods. The results are given in Table 6 and Fig. 11.

As it is shown in Table 6 and Fig. 11, the AT process has the highest accuracy, then VRS-DG and at finally the RTK-DG. This is of course sensible and compliant with the common accuracy of both VRS and RTK.

Table 6
Accuracy of AT and DG by linear EO parameters as determined by RTK and VRS techniques defined as total points RMSE.

Pts	Total points RMSE		
	AT by GCPs determined by static GNSS	DG by linear OE parameters determined by	
		RTK	VRS
point8	0.010	0.030	0.030
point9	0.022	0.016	0.022
point10	0.029	0.023	0.029
point11	0.022	0.019	0.015
point13	0.023	0.033	0.022
point15	0.013	0.048	0.043
point17	0.015	0.069	0.054
point19	0.009	0.035	0.028
Total	0.019	0.045	0.039

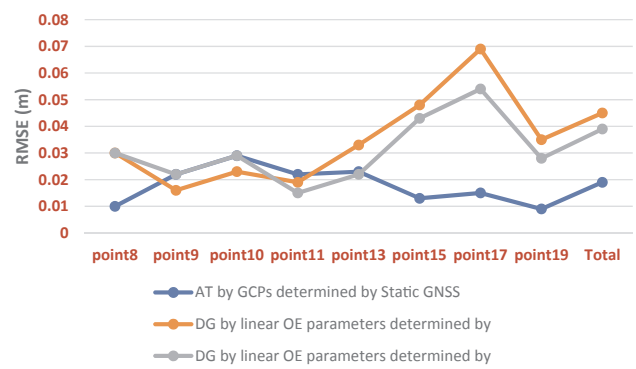

Fig. 11. Comparison between accuracy of AT and DG by linear EO parameters determined by RTK and VRS techniques.

4. Conclusions

The study has demonstrated that classical AT is more accurate than the UAV imagery DG. Direct Geo-referencing method has ability to provide products in good accuracy. Using VRS and RTK in determining the linear EO parameters in direct geo-referencing give a suitable accuracy enough to do the sequence processing. The accuracies achieved for VRS-DG and RTK-DG were 0.029 & 0.034 horizontal RMSE and 0.026 and 0.029 m for vertical RMSE. On the other side, the accuracy for AT horizontal RMSE was 0.014 m and 0.013 m vertical RMSE.

Acknowledgment

We would like to thank and acknowledge the sense fly company for providing the Photogrammetric dataset and supporting us in this paper.

References

Agisoft, 2017. Agisoft PhotoScan User Manual: Professional Edition, Version1.3.0. < http://www.agisoft.com/pdf/photoscan-pro_1_3_en.pdf > .

Barnhart, T.B., Crosby, B.T., 2013. Comparing two methods of surface change detection on an evolving thermokarst using high-temporal-frequency terrestrial laser scanning, Selawik River, Alaska. Remote Sens. 5, 2813–2837.

Cramer, M., Stallmann, D., Haala, N., 2000. Direct geo-referencing using GPS/inertial exterior orientations for photogrammetric applications. International Archives of Photogrammetry and Remote Sensing, Amsterdam, The Netherlands, Vol. 33, Part B3, pp. 198–205.

Cramer, M., Stallmann, D., 2002. System calibration for direct georeferencing, international archives of photogrammetry. Remote Sensing and Spatial Information Sciences, 34(3/A), pp. 79–84.

FGDC, 1998. Geospatial Positioning Accuracy Standards. FGDC-STD-007.3-1998, Part 3:

National Standard for Spatial Data Accuracy (NSSDA).

Gross, J.W., Heumann, B.W., 2016. A statistical examination of image stitching software packages for use with unmanned aerial systems. Photogramm. Eng. Remote Sens. 82 (6), 419–425.

Gross, J.W., 2015. A comparison of orthomosaic software for use with ultra high-resolution imagery of a wetland environment. Center for Geographic Information Science and Geography Department.

Jacobsen, K., 2002. Calibration aspects in direct georeferencing of frame imagery. Pecora 15/Land Satellite Information, Denver, USA, pp. 82–88.

Li, X.Y., 2005. Principle, method and practice of IMU/DGPS based photogrammetry. Information Engineering University, Zhengzhou, China.